A SIMPLE TECHNIQUE FOR OPTIMIZING THE IMPLEMENTATION OF THE APERTURE THEOREM BASED ON EQUIVALENCE PRINCIPLE

S. Qiu[*], Y. Lu, N. Liu, and P. Li

Department of Electrical Engineering, Beijing University of Posts and Telecommunications, Beijing 100876, China

Abstract—The electromagnetic characteristic of the aperture located on a PEC (Perfect Electric Conductor) cavity is an important and challenging research in CEM (Computational Electromagnetics) and practical applications. Researches have been done well when the apertures located on a large flat surface. But the complex slots and apertures are still difficult to analyze, such as a thin long slot. The thin long slots present on different kinds of structures, such as missiles, aircrafts, handset equipments, and computers. In addition, most of the surfaces are non-flat. Furthermore, the multiscale characteristic of the structure makes the modeling very difficult in such cases. It becomes an increasing interesting research recently. A better result can be obtained by generating much more denser meshes. Because of the complexity of the algorithm and the ill-posed matrix problem, it is not an optimized option. In order to get a better use of the aperture theorem in the multiscale problems, a separation technique is developed in this paper. By using the readjustment of the equivalent electric and magnetic currents, a simplified model is proposed. Arbitrary shaped aperture can be very well handled through this method, especially the thin long slots.

1. INTRODUCTION

HE electromagnetic scattering of the multiscale structures attracts great attention in the recent studies. The equivalence principle is a useful theorem in these problems. The electromagnetic translation of the aperture is also an important electromagnetic phenomenon in such

a multiscale problem. The classical aperture theorem is used when
there are apertures. Using the aperture theorem, an aperture located
on the infinite large plane is solved by Harrington and Mautz [1] in
the beginning. Then, many other cases are studied [2–8]. The shape
and depth of the aperture are the main concern. But, the apertures
always present on an electric large and flat PEC surface. Wang et
al. [9] extends the aperture theorem to an arbitrary shaped aperture
on an arbitrary shaped PEC cavity. The fields change rapidly in
the vicinity of the aperture. And it changes faster when there are
multiscale apertures. Denser meshes are needed to capture the induced
electric and equivalent magnetic currents. The situations are worse
when the shapes are not regular. Sometimes it is hardly possible, such
as a thin long slot. Recently, the TSF(Thin-Slot Formula) [10–14]
technique is developed based on the FDTD method. As well-known,
the Yee cells cannot model the non-regular shapes very well. The TSF
technique is only for the long thin slot. It can be a problem when
it is used in the multiscale structures. The equivalence principle is
introduced to increase the accuracy of the results in [14]. But because
the denominators of the coefficient in the updating equations contain
the electric fields which are zero in some moments in the simulation,
it is not easy to use in practice. And the slot needs to be just in
the center of the Yee cell in the TSF technique. And the results
become inaccurate when the width of the slot equals the length of the
cell's edge. When using other numerical methods alone, such as FEM
and MOM, much denser meshes are needed in the aperture region.
And it often results in an ill-posed matrix. The aperture theorem
which utilizes the equivalence principle is exact. But the numerical
manipulation will always bring errors. The equivalent currents are
discussed, and then a simplified model is proposed in this paper. The
method can be easily used in the multiscale structures. And the thin-
slot can be well handled by this method.

2. APERTURE THEOREM AND THE SEPARATION TECHNIQUE

2.1. Classical Aperture Theorem

The aperture theorem is based on the equivalence principle. The detail
of the equivalence principle is described by Harrington in his book [15].
Because many surfaces can be the equivalent surfaces, there are lots
kinds of the equivalent currents. Theoretically, the different choices
do not lead to different results. Because of the numerical process,
bigger errors would present when the improper surface is chosen in
numerical simulations. The degree of accuracy depends on how exactly

the equivalent currents on the imagine surface are modeled. A classical configuration of the problem is shown in Fig. 1(a). The problem is to solve for the fields in V_1 and V_2, which are separated by the surface S. The V_1 surrounds V_2, and extends to the infinity. The constitutive parameters are complex values, (ε_1, μ_1) in V_1 and (ε_2, μ_2) in V_2. The sources inside region 1 (V_1) are $(\mathbf{J}_1, \mathbf{M}_1)$. And $(\mathbf{E}_1, \mathbf{H}_1)$ are the total fields in region 1. The quantities in region 2 (V_2) are denoted by simply changing the subscripts 1 to 2. The boldface characters represent vectors in this paper. In order to get the matrix equations, the procedure of the aperture theorem is divided into two steps. Each step results in an equivalent problem. First step, by using the equivalence principle once, the original problem is divided into two equivalent problem as shown in Figs. 1(b) and (c). They are the outer and inner problems. The equivalent surfaces are S^+ and S^-. It is zero fields which are shown in Fig. 1(b) in region 2, but real fields in Fig. 1(c). Then, the "short-circuit" technique is introduced in the second step. The above two equivalent problems become two new problems. In these new equivalent problems, the surface S becomes a completely
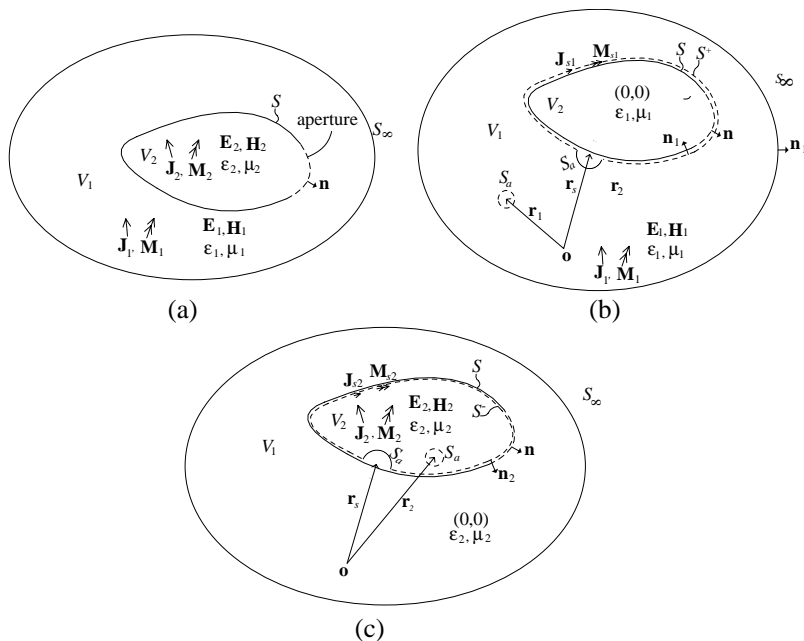

Figure 1. Problems in aperture theorem.

sealed PEC surface, under the real sources and equivalent currents'
illumination. But the equivalent electric currents are cancelled out,
leaving only equivalent magnetic currents. When the surface S is
electrically large and flat, the image theory can be used to further
simplify the problems. But the approximation is introduced when S is
finite or curved. Next, by utilizing the boundary conditions over the
aperture and using the equivalence principle again, integral equations
are derived. In fact, although the second step is an option when the
PEC surface is not infinite large and flat, it still works well except that
we can not use the image theory to further simplify the problems here.
In the aperture theorem, the equivalent magnetic currents which only
exist on the aperture surface are solved first, and then the outer and
inner surface electric currents.

2.2. The Separation Technique

The results are almost exact as mentioned above. The more precise
results are realized through introducing denser meshes in the multiscale
problems. But it is hardly enough in some special geometries, such as
the thin long slots. In order to overcome this difficulty, we introduce
a separation technique by analyzing the equivalent currents over the
aperture region. In the classical aperture theorem, the short-circuit
technique is used after the first step. Because of the PEC boundary
condition, the tangential electric fields need to be zeros on the surface.
But it is not true in the model. So, Booysen [16] questions the
procedure. And then he states that there should be a small gap
between S and the equivalent surface S^+ and S^- [17]. However, they
are treated as the same during the calculation in order to stick to the
boundary conditions. The published literatures adopt this concept,
using the model which states that the magnetic currents exit on the
PEC surface and the same meshes for both equivalent currents. The
validation of the calculation and experimental results can be found
in [7] and [17]. In these papers, the authors use the calculation methods
including FDTD and the MOM.

Following, as shown in the Fig. 2, we separate the equivalent
electric and magnetic currents just after the first step. Now, the same
or different meshes can be used. In Fig. 2, h means the distance of the
two equivalent currents over the aperture region, namely the distance
between S_1 and S_{AP} or S_2 and S_{AP}. And they are not necessarily
equal. The S_{AP} is the surface of the aperture. The S_{PEC} denotes
the PEC surface of the original problem. Now, the equivalent electric
currents are on S_{PEC} and S_{AP}, while equivalent magnetic currents
are on S_1 and S_2. However, the boundary conditions are broken
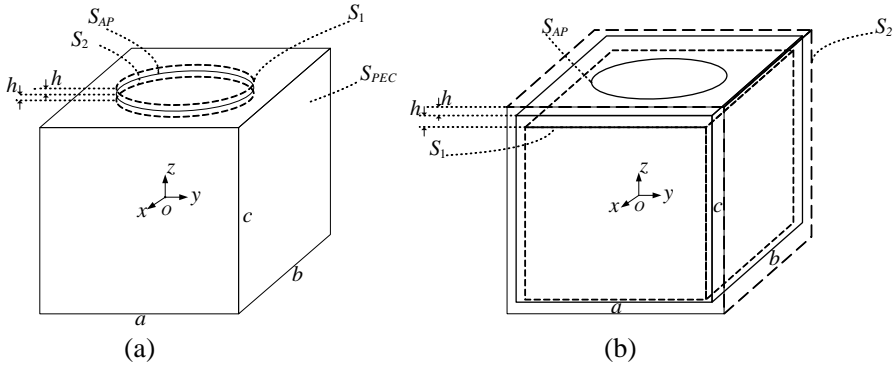down. From another point of view, all sources including the real and

Figure 2. Separation of the equivalence currents.

equivalent sources are radiating in a free space in these equivalent problems. The separation can be viewed as a perturbation of the sources. There is a break of the equivalent magnetic currents over the aperture region. The currents suddenly change from some finite values to zero. This results in rapid changes of the fields in the vicinity of the aperture. In turn, we conclude that the equivalent magnetic currents would change drastically with different h. The evident results are seen in the numerical simulations. It seems difficult to determine the distance h here. In fact, h falls in a quite large range. Next, we perform the second step. The final equivalent problem is shown in the Figs. 2(a) or (b), with the aperture closed by a PEC surface here. There are two ways to separate the equivalent currents. One is just to move equivalent magnetic currents as shown in Fig. 2(a), and the other is to move electric currents as shown in Fig. 2(b). No differences of the results should be found between these two methods theoretically. The magnetic currents move into the analyzing zone in the first method. While moving the equivalent electric currents, the analyzing zone is enlarged. Because of the bigger perturbation of the resonant frequency of the cavity, it results in bigger errors in numerical simulations when the frequency is near the resonant frequency. And because the equivalent magnetic currents are h away from the PEC surface in Fig. 2, there are image magnetic currents. These image currents are distorted when the PEC surface is non-infinite or non-flat. And these two currents always generate zero electric fields on the PEC surface. This makes the value of h fall in a large range.

3. FORMULATIONS AND MOMENT PROCEDURE

3.1. Integral Equations

In this section, integral equations are derived using the equivalence principle. It turns out to be that, it does not need such a compensated current in [9]. It must be an electric current induced on the PEC's surfaces. And because the doubly image theory can not be used in these cases when the PEC surface is electrically small or curved, we derive the integral equations without using image theory below. The magnetic current which is just outside an electric current sheet would induce an image, no matter what shape of the electric current sheet is. But the image is distorted when the sheet is electrically small or not flat.

For simplicity, the sources ($\mathbf{E}^{inc}$, $\mathbf{H}^{inc}$) are only in V_1. $\mathbf{n}$ is the outward unit normal vector of the surface S from V_2. The two equivalent problems are drawn in one figure, as shown in Fig. 3. In the figure, equivalent electric currents are on the outer and inner surfaces of the cavity surface. Equivalent magnetic currents are separated from the cavity. We use the MOM (method of moment) in this paper. The integral equations are used in the numerical analysis. Following the process in [18], the electromagnetic fields on the inside and outside surfaces of the PEC cavity are:

$$\mathbf{E}^1(\mathbf{r}) = 2\mathbf{E}^{inc} + 2\int_{s+}\left[-j\omega\mu_1\mathbf{J}_{s1}g_1 - \mathbf{M}_{s1}\times\nabla'g_1\right.$$
$$\left. -(1/j\omega\varepsilon_1)(\nabla'\cdot\mathbf{J}_{s1})\nabla'g_1\right]ds' \tag{1}$$
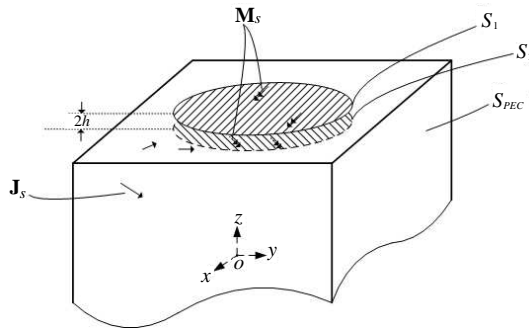

Figure 3. Geometry of equivalence currents on the aperture.

$$\mathbf{H}^1(\mathbf{r}) = 2\mathbf{H}^{inc} + 2 \int_{s+} \Big[-j\omega\varepsilon_1 \mathbf{M}_{s1} g_1 + \mathbf{J}_{s1} \times \nabla' g_1$$

$$-(1/j\omega\mu_1)(\nabla' \cdot \mathbf{M}_{s1})\nabla' g_1 \Big] ds' \tag{2}$$

$$\mathbf{E}^2(\mathbf{r}) = 2 \int_{s-} [-j\omega\mu_2(-J_{s2})g_2$$

$$-(-\mathbf{M}_{s2}) \times \nabla' g_2 - (1/j\omega\varepsilon_2)(\nabla' \cdot (-\mathbf{J}_{s2}))\nabla' g_2] ds' \tag{3}$$

$$\mathbf{H}^2(\mathbf{r}) = 2 \int_{s-} [-j\omega\varepsilon_2(-\mathbf{M}_{s2})g_2 + (-\mathbf{J}_{s2}) \times \nabla' g_2$$

$$-(1/j\omega\mu_2)(\nabla' \cdot (-\mathbf{M}_{s2}))\nabla' g_2] ds' \tag{4}$$

where $g_x = e^{-jk_x R}/4\pi R$, $R = |\mathbf{r} - \mathbf{r}'|$, k_x is the wave number of the material in region 1 or 2, $\mathbf{J}_{s,1/2}$ and $\mathbf{M}_{s,1/2}$ are the outside or inside surface currents which are defined as:

$$\mathbf{J}_{s1/2} = \mathbf{n} \times \mathbf{H}^{1/2} \tag{5}$$

$$\mathbf{M}_{s1/2} = \mathbf{E}^{1/2} \times \mathbf{n} \tag{6}$$

Note that, we use the same unit normal vector when the currents are on the outer or inner surface in (5) and (6). By substituting the bellow notations:

$$\mathbf{E}(\mathbf{J}_s) = \int_s \Big[-j\omega\mu\mathbf{J}_s g - (1/j\omega\varepsilon)(\nabla' \cdot \mathbf{J}_s)\nabla' g \Big] ds' \tag{7}$$

$$\mathbf{E}(\mathbf{M}_s) = \int_s \Big[\mathbf{M}_s \times \nabla' g \Big] ds' \tag{8}$$

$$\mathbf{H}(\mathbf{J}_s) = \int_s \Big[\mathbf{J}_s \times \nabla' g \Big] ds' \tag{9}$$

$$\mathbf{H}(\mathbf{M}_s) = \int_s \Big[-j\omega\varepsilon\mathbf{M}_s g - (1/j\omega\mu)\left(\nabla' \cdot \mathbf{M}_s\right)\nabla' g \Big] ds' \tag{10}$$

into (1)–(4), we get:

$$\mathbf{E}^1(\mathbf{r}) = 2\mathbf{E}^{inc} + 2\mathbf{E}^1(\mathbf{J}_{s1}) - 2\mathbf{E}^1(\mathbf{M}_{s1}) \tag{11}$$

$$\mathbf{H}^1(\mathbf{r}) = 2\mathbf{H}^{inc} + 2\mathbf{H}^1(\mathbf{J}_{s1}) + 2\mathbf{H}^1(\mathbf{M}_{s1}) \tag{12}$$

$$\mathbf{E}^2(\mathbf{r}) = 2\mathbf{E}^2(-\mathbf{J}_{s2}) - 2\mathbf{E}^2(-\mathbf{M}_{s2}) \tag{13}$$

$$\mathbf{H}^2(\mathbf{r}) = 2\mathbf{H}^2(-\mathbf{J}_{s2}) + 2\mathbf{H}^2(-\mathbf{M}_{s2}) \tag{14}$$

Applying the boundary conditions of the electric fields on the outer and inner sides of the cavity, we have:

$$0 = [\mathbf{E}^{inc} + \mathbf{E}_1(\mathbf{J}_{s1}) - \mathbf{E}_1(\mathbf{M}_{s1})]_{\tan} \tag{15}$$

$$0 = [\mathbf{E}_2(-\mathbf{J}_{s2}) - \mathbf{E}_2(-\mathbf{M}_{s2})]_{\tan} \tag{16}$$

where $[\ldots]_{\text{tan}}$ means the tangential components. There are four unknown variables in the integral equations. Another two equations can be derived using the electric and magnetic boundary conditions on the aperture. When the aperture is thick and has complex shape, the complexity of the equations increases greatly. A lot of simplified methods are developed. The discussions and comparisons can be found in [19]. An other classical method, which is called local transmission line theory, is developed by Warne and Chen [8]. The mode matching also is a useful technique for connecting the inside and outside region. Most recently, the authors use this technique to analyze a rectangular aperture located on a rectangular cavity in [20]. But it is limited to regular shapes. Because we focus on the separation technique, a thin aperture is assumed in this paper. However, it is necessary to introduce the local transmission line theory in this technique in the next studies. So, in the aperture region:

$$\mathbf{n} \times \mathbf{E}^1(\mathbf{r}) = \mathbf{n} \times \mathbf{E}^2(\mathbf{r}) \tag{17}$$

$$\mathbf{n} \times \mathbf{H}^1(\mathbf{r}) = \mathbf{n} \times \mathbf{H}^2(\mathbf{r}) \tag{18}$$

Then, the other two equations are:

$$\mathbf{M}_{s1} = \mathbf{M}_{s2} \tag{19}$$

$$\mathbf{n} \times [\mathbf{H}^{inc} + \mathbf{H}^1(\mathbf{J}_{s1}) + \mathbf{H}^1(\mathbf{M}_{s1})] = \mathbf{n} \times [-\mathbf{H}^2(\mathbf{J}_{s2}) - \mathbf{H}^2(\mathbf{M}_{s2})] \tag{20}$$

3.2. The Moment Procedure

Firstly, the cavity and aperture's surfaces are divided into many triangular patches. Then equivalent currents $\mathbf{J}_s$ and $\mathbf{M}_s$ are expanded by the same basic functions $\mathbf{J}_n$ over the patches. And the equivalent magnetic currents are expanded as:

$$\mathbf{M}_s = \mathbf{M}_{s1} = \mathbf{M}_{s2} = \sum_{n=1}^{N_A} v_n \mathbf{M}_n \tag{21}$$

where N_A is the number of basic functions on the equivalent surface S_A (the aperture surface), $\mathbf{M}_n = \mathbf{J}_n$, and the v_n is the unknown coefficient.

$$\mathbf{J}_{s1} = \sum_{n=1}^{N} I_n^1 \mathbf{J}_n \tag{22}$$

$$\mathbf{J}_{s2} = \sum_{n=1}^{N} I_n^2 \mathbf{J}_n \tag{23}$$

where N is the number of basic functions on the sealed PEC surface, I_n is the unknown coefficient. The electric currents are continuous across

the whole surface, and the magnetic currents are still considered to be continuous but changes rapidly from nonzero to zero when crossing the edge of the aperture. Define the vector symmetric inner product as:

$$< \mathbf{a}, \mathbf{b} >= \int_s (\mathbf{a} \cdot \mathbf{b}) ds \qquad (24)$$

where $\mathbf{a}$ and $\mathbf{b}$ are vectors. Substituting (21) and (22) into (15), and testing with $\mathbf{J}_m$, we have:

$$0 = < \mathbf{J}_m, \ \mathbf{E}^{inc} > + \sum_{n=1}^{N} I_n^1 < \mathbf{J}_m, \ \mathbf{E}(\mathbf{J}_n) > - \sum_{n=1}^{N_A} v_n < \mathbf{J}_m, \mathbf{E}(\mathbf{M}_n) > \quad (25)$$

where $m = 1 \dots N$. The tangential subscripts of the fields are dropt. Similarly, testing (16) with $\mathbf{J}_m$, we get:

$$0 = - \sum_{n=1}^{N} I_n^2 < \mathbf{J}_m, \ \mathbf{E}(\mathbf{J}_n) > + \sum_{n=1}^{N_A} v_n < \mathbf{J}_m, \ \mathbf{E}(\mathbf{M}_n) > \qquad (26)$$

where $m = 1 \dots N$. The cross product of Equation (20) can be changed to dot product by introducing an arbitrary tangential vector $\mathbf{t}(\mathbf{r})$ on the aperture surface:

$$\mathbf{t}(\mathbf{r}) \cdot [\mathbf{H}^{inc} + \mathbf{H}(\mathbf{J}_{s1}) + \mathbf{H}(\mathbf{M}_{s1})] = \mathbf{t}(\mathbf{r}) \cdot [-\mathbf{H}(\mathbf{J}_{s2} - \mathbf{H}(\mathbf{M}_{s2})] \quad (27)$$

Now, testing (27) with $\mathbf{J}_m$, $\mathbf{t}(\mathbf{r})$ can be replaced by $\mathbf{J}_m$. Then:

$$< \mathbf{J}_m, \mathbf{H}^{inc} > + \sum_{n=1}^{N} I_n^1 < \mathbf{J}_m, \mathbf{H}(\mathbf{J}_n) > + \sum_{n=1}^{N_A} v_n < \mathbf{J}_m, \mathbf{H}(\mathbf{M}_n) >$$

$$= - \sum_{n=1}^{N} I_n^2 < \mathbf{J}_m, \mathbf{H}(\mathbf{J}_n) > - \sum_{n=1}^{N_A} v_n < \mathbf{J}_m, \mathbf{H}(\mathbf{M}_n) > \qquad (28)$$

Because (27) is only correct on the aperture, in (28) $m = 1 \dots N_A$. With Equations (25), (26) and (28), the unknown coefficients can be solved. Matrix representations are:

$$0 = [V_m^E]_N + [Z_{mn}^{EJ}]_{N \times N}[I_n^1]_N - [Z_{mn}^{EM}]_{N \times N_A}[v_n]_{N_A} \qquad (29)$$

$$0 = -[Z_{mn}^{EJ}]_{N \times N}[I_n^2]_N + [Z_{mn}^{EM}]_{N \times N_A}[v_n]_{N_A} \qquad (30)$$

$$[V_m^H]_{N_A} + [Z_{mn}^{HJ}]_{N_A \times N}[I_n^1]_N + [Z_{mn}^{HM}]_{N_A \times N_A}[v_n]_{N_A}$$

$$= -[Z_{mn}^{HJ}]_{N_A \times N}[I_n^2]_N - [Z_{mn}^{HM}]_{N_A \times N_A}[v_n]_{N_A} \qquad (31)$$

The elements of (29), (30), (31) are:

$$V_m^E = < \mathbf{J}_m, \mathbf{E}^{inc} > \qquad (32)$$

$$V_m^{\mathrm{H}} = <\mathbf{J}_m, \mathbf{H}^{inc}> \tag{33}$$

$$Z_{mn}^{EJ} = <\mathbf{J}_m, \mathbf{E}(\mathbf{J}_n)> \tag{34}$$

$$Z_{mn}^{EM} = <\mathbf{J}_m, \mathbf{E}(\mathbf{M}_n)> \tag{35}$$

$$Z_{mn}^{HJ} = <\mathbf{J}_m, \mathbf{H}(\mathbf{J}_n)> \tag{36}$$

$$Z_{mn}^{HM} = <\mathbf{J}_m, \mathbf{H}(\mathbf{M}_n)> \tag{37}$$

Because $\mathbf{M}_n = \mathbf{J}_n$ in this paper, and noticing (7)–(10), so that:

$$Z_{mn}^{HM} = Z_{mn}^{EJ}/\eta^2 \tag{38}$$

$$Z_{mn}^{EM} = Z_{mn}^{HJ} \tag{39}$$

where η is the intrinsic impedance of the medium. The matrix equations can be used to solve for v_n firstly, and then I_n can be obtained through (29) and (30). In the above equations, we no longer distinguish the inside or outside surfaces. And it should be aware of the evaluation of the elements when the sources are separated. Two types of matrix elements need to be evaluated.

It has been proved that arbitrary shape objects can be modeled by planar triangular patches very well. The typical expansion function named RWG [21] is used, in which $\mathbf{J}_n$ is defined on each inner edge between two patches:

$$\mathbf{J}_n(\mathbf{r}) = \begin{cases} \frac{l_n}{2A_n^+}\boldsymbol{\rho}_n^+, & \mathbf{r} \text{ in } T_n^+ \\ \frac{l_n}{2A_n^-}\boldsymbol{\rho}_n^-, & \mathbf{r} \text{ in } T_n^- \\ 0, & \text{elsewhere} \end{cases} \tag{40}$$

where l_n is the nth edge's length; T^+ and T^- are the plus and minus triangular patches of the nth edge respectively, and A^+ and A^- are the triangle's area. Let $\mathbf{v}^+$ and $\mathbf{v}^-$ are defined as the free vertex vectors of the edges. So,

$$\boldsymbol{\rho}_n^+ = \mathbf{r} - \mathbf{v}^+ \tag{41}$$

$$\boldsymbol{\rho}_n^- = -\mathbf{r} + \mathbf{v}^- \tag{42}$$

Since the accuracy of the results in MOM simulations closely depends on the evaluation of the matrix elements, we consider the process carefully. In fact, the significant factor is the accuracy of the elements which are located on the diagonal line of the matrix. They are highly affected by the calculation method as shown in a lot of published literatures. It occurs when the testing and source points are in a same triangular patch. The analytical and numerical evaluations of the singular term in the testing procedure are extensively studied [22–27]. Typical singularity extractions can be found in [22–23]. And they

are used in this paper. Suppose the incident fields ($\mathbf{E}^{inc}$, $\mathbf{H}^{inc}$),

$$\mathbf{E}^{inc} = \mathbf{E}_0 e^{-j\mathbf{k}\cdot\mathbf{r}} \qquad (43)$$

$$\mathbf{H}^{inc} = (1/\eta)\hat{\mathbf{k}} \times \mathbf{E}^{inc} \qquad (44)$$

where $\mathbf{k}$ is the propagation vector.

3.3. Numerical Example

For no loss of generality, the magnetic currents separation is used in following example. The shape of the aperture is circle. Obviously, it goes the same way when the separation technique is used in the thin long slot case. A cubic PEC cavity is assumed to have the edge length of 0.0796 m. And the shape of the aperture is a circle with 0.0398 m as its diameter. And the thickness of the cavity is 0.002 m. The points A and B are selected as the testing fields' points which are shown in Fig. 4. The equivalent magnetic currents are pulled away from aperture surface S_{AP}. It is supposed that a plane wave illuminates from $+z$, and $+x$ polarizing in this simulation.

The scattering electric fields and the RCS are compared in Fig. 5 and Fig. 6. And $h = dl_{\min}$, where $l_{\min}$ is the minimum length of triangle patch's edge, which is 0.0031 m in this simulation. From the figures, we can see that the fields and the RCS are almost the same when d is at different values. The results agree well with that calculated by CST. But there is big difference between results calculated by HFSS and our codes. The difference is mainly due to the thickness of the cavity
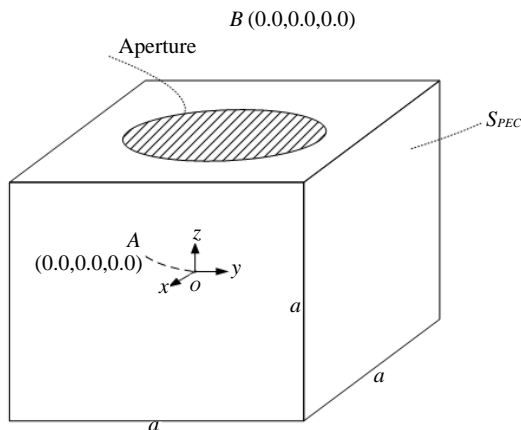

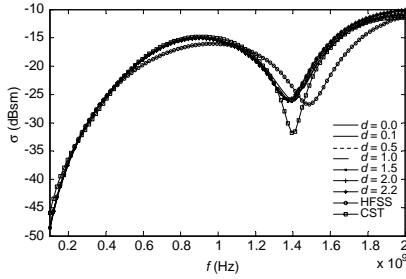**Figure 4.** Configuration of the aperture and cavity.

Figure 5. Bistatic RCS of the aperture with different separating distance.
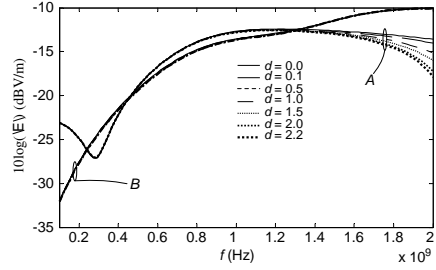
Figure 6. Scattering electric fields at point A and B.

we used in the HFSS' simulation. The inner scattering electric fields tend to far from each other for different value of d when the frequency increases. But it converges when h tends to zero as shown in Fig. 6. It is expected that the divergence arises since the equivalent currents can be viewed as a perturbation when the scattering fields inside the cavity are calculated. The bigger the perturbation the larger difference appears. In order to get an accurate result, the distance d is selected at a proper value. But it falls in a relatively large range as discussed above. A deeper discussion of the performance and applications of the method is included in the coming paper. In the contrary, the electric fields outside the cavity vary little with different value of d.

4. CONCLUSION

The procedure of the aperture theorem is studied in this paper. And the equivalent currents are discussed, especially that over the aperture region. Then, a separation technique is used and analyzed. The technique utilizes the approximation of the boundary conditions. Owing to the images of the equivalent magnetic currents, the value of the separating distance falls in a large range. And it can be different values in different regions. Because of the separation of the equivalent electric and magnetic currents, the meshes of the closed PEC surface and the equivalent magnetic currents can be considered separately. This makes the implementation of the thin long slot easily. The PEC cavity can be viewed as closed, while the thin long slot can be modeled as the thin line in a worst case. It is worth mentioning that when the separation distance becomes zero, the classical aperture theorem is revised.

ACKNOWLEDGMENT

REFERENCES

1. Harrington, R. and J. Mautz, "A generalized network formulation for aperture problems," *IEEE Trans. Antennas Propag.*, Vol. 24, 870–873, Nov. 1976.

2. Auckland, D. T. and R. F. Harrington, "Electromagnetic transmission through a filled slit in a conducting plane of finite thickness, TE case," *IEEE Trans. Microwave Theory and Techniques*, Vol. 26, 499–505, Jul. 1978.

3. Liang, C.-H. and D. Cheng, "Electromagnetic fields coupled into a cavity with a slot-aperture under resonant conditions," *IEEE Trans. Antennas Propag.*, Vol. 30, 664–672, Jul. 1982.

4. Harrington, R., "Resonant behavior of a small aperture backed by a conducting body," *IEEE Trans. Antennas Propag.*, Vol. 30, 205–212, Mar. 1982.

5. Harrington, R. and D. Auckland, "Electromagnetic transmission through narrow slots in thick conducting screens," *IEEE Trans. Antennas Propag.*, Vol. 28, 616–622, Sep. 1980.

6. Hsi, S., R. Harrington, and J. Mautz, "Electromagnetic coupling to a conducting wire behind an aperture of arbitrary size and shape," *IEEE Trans. Antennas Propag.*, Vol. 33, 581–587, Jun. 1985.

7. Umashankar, K., A. Taflove, and B. Beker, "Calculation and experimental validation of induced currents on coupled wires in an arbitrary shaped cavity," *IEEE Trans. Antennas Propag.*, Vol. 35, 1248–1257, Nov. 1987.

8. Warne, L. K. and K. C. Chen, "Equivalent antenna radius for narrow slot apertures having depth," *IEEE Trans. Antennas Propag.*, Vol. 37, 824–834, Jul. 1989.

9. Wang, T., R. F. Harrington, and J. R. Mautz, "Electromagnetic scattering from and transmission through arbitrary apertures in conducting bodies," *IEEE Trans. Antennas Propag.*, Vol. 38, 1805–1814, Nov. 1990.

10. Gilbert, J. and R. Holland, "Implementation of the thin-slot formalism in the finite-difference EMP code THREDII," *IEEE Trans. Nucl. Sci.*, Vol. 28, No. 6, 4269–4274, Dec. 1981.

11. Wu, C.-T., Y.-H. Pang, and R.-B. Wu, "An improved formalism for FDTD analysis of thin-slot problems by conformal mapping technique," *IEEE Trans. Antennas Propag.*, Vol. 51, No. 9, 2530–2533, Sep. 2003.

12. Gkatzianas, M. A., "The Gilbert-Holland FDTD thin slot model revisited: An alternative expression for the in-cell capacitance," *IEEE Microw. Wireless Compon. Lett.*, Vol. 14, No. 5, 219–221, May 2004.

13. Wang, B.-Z., "Enhanced thin-slot formalism for the FDTD analysis of thin-slot penetration," *IEEE Microw. Guided Wave Lett.*, Vol. 5, No. 5, 142–143, May 1995.

14. Xiong, R., B. Chen, Q. Yin, and Z.-Y. Cai, "Improved formalism for the FDTD analysis of thin-slot penetration by equivalence principle," *IEEE Antennas and Wireless Propagation Letters*, Vol. 10, 655–657, 2011.

15. Harington, R. F., *Time-Harmonic Electromagnetic Fields*, McGraw-Hill, New York, 1961.

16. Booysen, A. J., "Aperture theory and the equivalence theorem," *IEEE Antennas and Propagation Society International Symposium*, Vol. 2, 1258–1261, Aug. 1999.

17. Booysen, A. J., "Aperture theory and the equivalence principle," *IEEE Antennas and Propagation Magazine*, Vol. 45, 29–40, Jun. 2003.

18. Chen, K. M., "A mathematical formulation of the equivalence principle," *IEEE Trans. Microwave Theory and Techniques*, Vol. 37, 1576–1581, Oct. 1989.

19. Anastassiu, H. T., "A review of electromagnetic scattering analysis for inlets, cavities, and open ducts," *IEEE Trans. Antennas Propag.*, Vol. 45, 27–40, Dec. 2003.

20. Wu, G., X. G. Zhang, and B. Liu, "A hybrid method for predicting the shielding effectiveness of rectangular metallic enclosures with thickness apertures," *Journal of Electromagnetic Waves and Applications*, Vol. 24, Nos. 8–9, 1157–1169, 2010.

21. Rao, S., D. Wilton, and A. Glisson, "Electromagnetic scattering by surfaces of arbitrary shape," *IEEE Trans. Antennas Propag.*, Vol. 30, 409–418, May 1982.

22. Wilton, D., S. Rao, A. Glisson, D. Schaubert, O. Al-Bundak, and C. Butler, "Potential integrals for uniform and linear source distributions on polygonal and polyhedral domains," *IEEE Trans. Antennas Propag.*, Vol. 32, 276–281, May 1984.

23. Hodges, R. E. and Y. Rahmat-Sarnii, "Evaluation of MFIE integrals with the use of vector triangle basis functions," *Microwave and Optical Technology Letters*, Vol. 14, No. 1, 9–14, Jan. 1997.

24. Caorsi, S., D. Moreno, and F. Sidoti, "Theoretical and numerical treatment of surface integrals involving the free-space Green's function," *IEEE Trans. Antennas Propag.,* Vol. 41, 1296–1301, Sep. 1993.

25. Graglia, R. D., "On the numerical integration of the linear shape functions times the 3-D Green's function or its gradient on a plane triangle," *IEEE Trans. Antennas Propag.*, Vol. 41, 1448–1455, Oct. 1993.

26. Sievers, D., T. F. Eibert, and V. Hansen, "correction to 'on the calculation of potential integrals for linear source distributions on triangular domains'," *IEEE Trans. Antennas Propag.*, Vol. 53, 3113, Sep. 2005.

27. Ogdanov, F. G., R. G. Jobava, and S. Frei, "About evaluation of the potential integrals for near field calculations in MoM solution to EFIE for triangulated surfaces, Direct and inverse problems of electromagnetic and acoustic wave theory," *Proceedings of the 7th International Seminar/Workshop on DIPED*, 113–117, 2002.